UNIVERSITY OF TWENTE.

Faculty of Engineering Technology

Sand-mud morphodynamic modeling in the coastal environment

Literature report

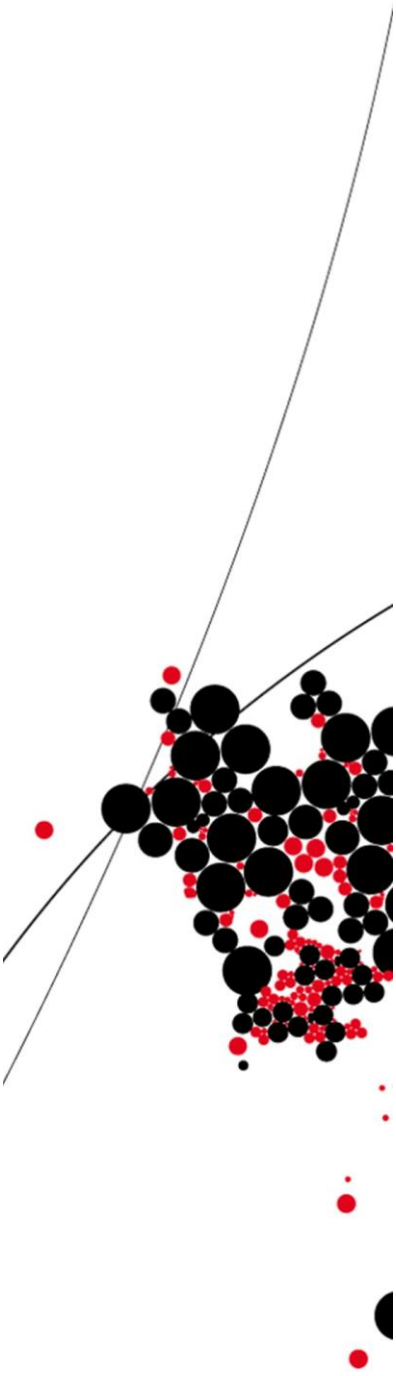

Paterno S. Miranda IV, MCE

January 2025

CE&M research report 2025R-001/WEM-001
ISSN 1568-4652

Literature report:

SAND-MUD MORPHODYNAMIC MODELING IN THE COASTAL ENVIRONMENT

Paterno S. Miranda IV, MCE

January 2025

Supervisors:
prof. dr. S.J.M.H. Hulscher
dr. ir. J.J. van der Werf

Marine and Fluvial Systems
University of Twente

CE&M research report 2025R-001/WEM-001
ISSN 1568-4652

TABLE OF CONTENTS

1. INTRODUCTION

1.1. BACKGROUND ON THE PHD PROJECT AND SAND-MUD

This PhD project is under the Sediment Transport and Morphodynamics in Marine and Coastal Waters with Engineering Solutions or SEDIMARE project (Grant Agreement No. 101072443) and is supported by the European Union's Horizon Europe Framework Programme via the Marie Skłodowska-Curie Actions Doctoral Network (HORIZON-MSCA-2021-DN-01). The objective of the SEDIMARE project is interdisciplinary training in coastal processes and engineering that is aimed at the sustainable use and protection of the coastal area. SEDIMARE is comprised of 3 work packages that are divided among 12 Doctoral Candidates. Each of these candidates focus on different aspects of sediment transport. This PhD project focuses on the transport of sand-mud from the numerical modeling perspective.

Estuaries are important bodies of water to sustain modern living. Most global ports around the world (e.g., Shanghai, China; Rotterdam, the Netherlands; Antwerp, Belgium) are constructed within an estuary. Estuaries also provide a unique ecosystem of flora and fauna that thrive in semi-inundated environments. Figure 1 shows examples of estuaries such as the port of Rotterdam and the Yangtze river estuary. Sand-mud beds can be found in estuaries. Understanding the dynamics of sand-mud beds becomes vital in maintaining and preserving the anthropogenic and natural systems present in estuaries. A common tool in the study of estuaries is the use of numerical models to simulate morphodynamic changes.

Figure 1. Port of Rotterdam (top) and Yangtze river estuary (bottom) (taken from Google Earth Pro)

1.2. NUMERICAL MODELING

Numerical simulation is ubiquitous in the analysis of morphodynamics. This is not only the case in an academic and research setting, but in engineering practice as well. Different numerical simulations seek to replicate processes occurring on different spatial and temporal scales.

Reynolds-averaged Navier-Stokes (RANS) models

At an intermediate length scales ($O\ 10^0$ m to 10^3 m), numerical models simulate processes but parameterize the small-scale processes using Reynolds-averaged values. Numerical models at this scale are called Reynolds-averaged Navier-stokes (RANS) models. In RANS models, some parameterizations include models for turbulence, by only considering the mean flow. Applying RANS models to morphodynamic simulations can produce morphodynamic evolution on the scale of years to decades.

Considering that morphodynamic modeling happens at intermediate length scales, the RANS models is the appropriate numerical simulation to use. The flexibility of RANS models to simulate bed evolution on time scales of years to decades reinforces this as the choice for morphodynamic modeling.

RANS morphodynamic models

Using RANS models, different knowledge institutions developed their own hydrodynamic and morphodynamic (or hydro-morphodynamic) coupled simulation software. In the morphodynamic modeling, these software have included non-cohesive and cohesive transport equations to help replicate the evolution of non-cohesive or cohesive beds, respectively. Examples of such software are Delft3D 4 and Delft3D FM (Deltares, 2023), TELEMAC-MASCARET (TELEMAC.org, 2023), and DHI Mike 21 (DHI, 2024).

The current morphodynamic software already include modules for sand-mud beds. These modules make use of the Partheniades formula for erosion flux but differ in their estimation of the critical bed shear stress, τ_{crit}, and the erosion parameter, M.

The recent literature to demonstrate sand-mud bed evolution was the work by Colina Alonso et al. (2023). This paper simulated long-term morphology and morphodynamics using an idealized Dutch Wadden Sea tidal basin. Colina Alonso made improvements to the critical bed shear stress and transport equations in Van Ledden (2003) and incorporated these into Delft3D. Delft3D also allows for user input to the critical bed shear stress and the erosion parameter.

In contrast, the published manuals of both TELEMAC (TELEMAC.org, 2022) and DHI Mike (DHI, 2024) do not have any set critical bed shear stress model but rely on user input or a static default value to estimate the erosion flux during sand-mud morphodynamic modeling.

Having discussed the need to study sand-mud systems and the availability of morphodynamic modeling suites, this literature review is done to understand the current state of sand-mud sediment morphodynamic modeling with a focus on RANS models. The following section poses literature questions that guide the search for current state-of-the-art and knowledge in this domain.

1.3. LITERATURE QUESTIONS

The literature questions follow a logical flow in the search for state-of-the-art knowledge in the field of sand-mud transport. The 1st question looks into the definition of sand-mud and where we can find this type of sediment. The 2nd question looks into the processes involved in sand-mud and seeks to gather mathematical formulations made to describe these processes. The final question wants to study the current morphodynamic model schemes used to simulate sand-mud bed evolution.

1. How to define sand-mud and what are systems that contain sand-mud?

2. What are the physical processes in sand-mud transport and which of these processes are modeled mathematically?
3. How is sand-mud bed evolution modeled in the RANS hydro-morphodynamic software, Delft3D in particular?

1.4. REPORT OUTLINE

The report structure will follow the flow of the literature questions.

Chapter 2 will describe sand-mud and its constituent parts. This chapter will also describe present systems that contain sand-mud with a brief description of the hydrodynamics and seabed sediment profile, and how some studies have modeled each system using a morphodynamic numerical model. Finally, a brief subchapter will also discuss how sand-mud systems around the world have been compared and contrasted.

Chapter 3 will discuss the processes involved in sand-mud transport. This overview will cover processes from erosion to the deposition of sand-mud from the seabed with an emphasis on the different mathematical models used to describe each process.

Finally, Chapter 4 will review the hydrodynamic and morphodynamic modeling scheme of Delft3D used for sand-mud systems. This chapter will focus on the numerical scheme implemented to parameterize near-bed exchange processes such as sediment fractions and the fluff layer module. The chapter will end by discussing literature that used Delft3D to simulate the evolution of sand-mud beds.

This literature review will end with a synthesis of the current knowledge on sand-mud transport by answering the questions defined from 1.3. Then, knowledge gaps will be identified in the current body of research.

2. DEFINITION OF SAND-MUD AND SYSTEMS CONTAINING SAND-MUD

Before reviewing the transportation of sand-mud, it is necessary to describe the composition of sand-mud and where sand-mud beds are located.

2.1. DEFINITION OF SAND-MUD AND ITS CONSTITUENT SEDIMENT CLASSES

Sand-mud is composed of the sediment classifications sand, clay, and silt. Sand is a non-cohesive particle. This means the transport of sand is governed by its size and weight. Conversely, clay is a cohesive particle. The transport of clay is governed by the electrochemical interactive forces between clay particles. Finally, silt is a non-cohesive particle that exhibits cohesion similar to clay. Due to the dual nature of silt, it is classified as apparently cohesive. Collectively, silt and clay are referred to as mud.

From the nature of each sediment class, a review of the size classification for each class can be performed. Dean & Dalrymple (2001) presents two sediment classifications: the Unified Soil Classification System (USCS) and the Wentworth scale size distribution (Wentworth).

The USCS classification was also adopted by the Japan Geotechnical Society (Yamada & Kobayashi, 2003). In this classification, particles are classified as sand if they have a diameter of 0.075 to 2 mm, as silt for particles of diameter 0.005 to 0.075 mm, and as clay for particles with diameters less than 0.005 mm. This classification is in line with the standard method of testing presented in ASTM D7928-21e1 (2021): Standard Test Method for Particle-Size Distribution (Gradation) of Fine-Grained Soils using the Sedimentation (Hydrometer) Analysis.

The Wentworth classification (Wentworth, 1922) was also similarly described by Van Ledden (2003) and presents scaling using an exponent of base 2. In this classification, sand is described as particles with diameter between 0.0625 to 2 mm, silt particles with diameter between 0.004 to 0.0625 mm, and clay particles with diameters less than 0.004 mm.

After looking at each of the sediment classes and their description, it is useful to look at how sediment compositions are presented. Sediment composition can be described in a ternary diagram. A sample ternary diagram is provided in Figure 2. This diagram is a triangle with sand, silt, and clay along each side of the triangle. Numbers along the sides of the triangle indicate the mass fraction of each sediment fraction. The direction of the tick marks indicates which direction the percentage of each sediment fraction runs along. For example, the round orange marker would be read as containing 50% sand, 20% silt, and 30% clay.

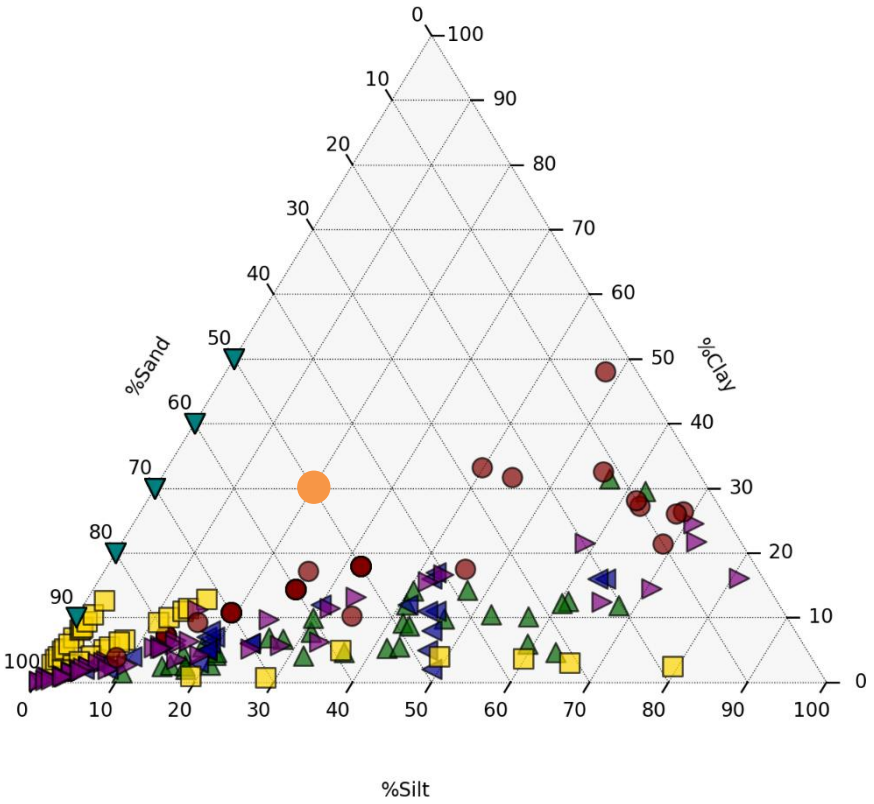

Figure 2. An empty ternary diagram with sample data from different sand-mud experiments. An orange round marker is also reflected to illustrate how to use and read a ternary diagram.

2.2. SYSTEMS WITH SAND-MUD

After providing a definition of sand-mud in the previous section, it is next necessary to identify systems where this type of sediment is present. These systems were selected because of the sediment characteristics, volume of research and availability of data. Each system will be given a brief description and will highlight some of its characteristics.

Scheldt estuary

The Scheldt estuary is situated between the Netherlands and Belgium (Figure 3). It serves as the passage to the port of Antwerp and has an estuary turbidity maximum (ETM) at its mouth that influences the sediment dynamics of the system (Fettweis et al., 2010; van Maren et al., 2020).

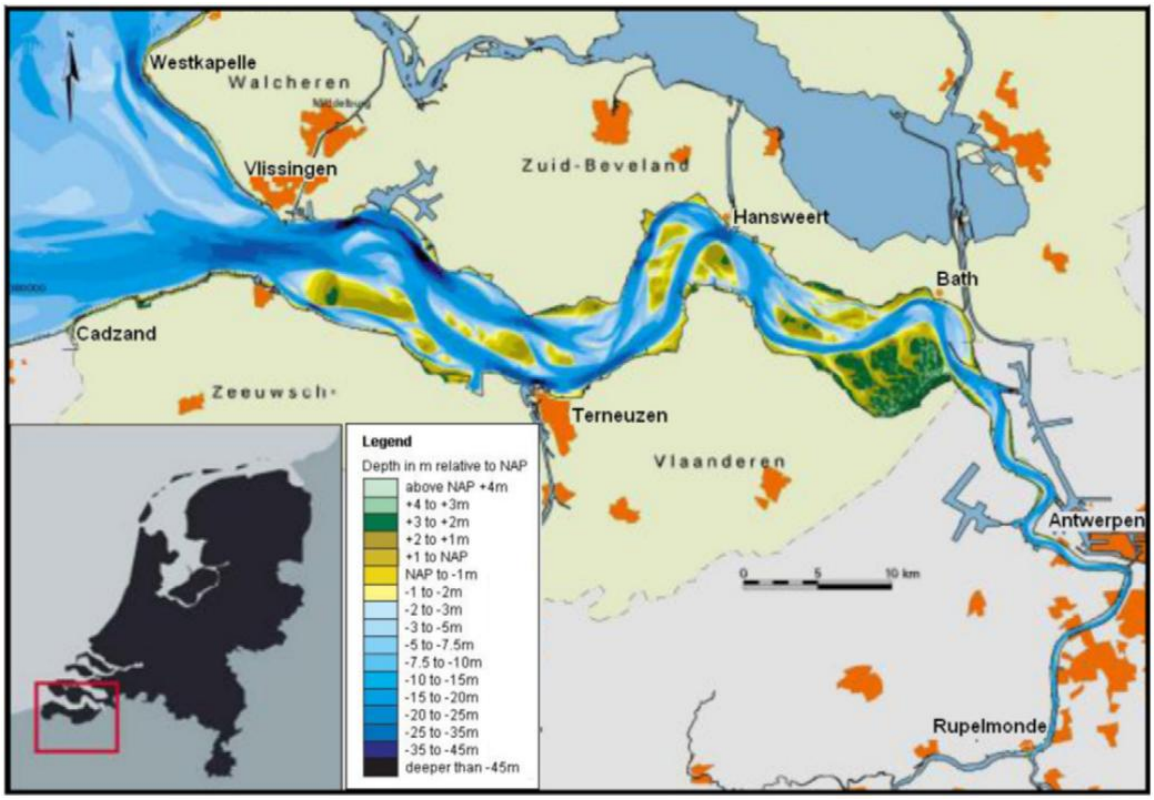

Figure 3. Vicinity map of the Scheldt estuary from Bolle et al. (2010) showing the bathymetry from the Antwerp to the mouth of the Scheldt estuary. The depths are referenced from NAP.

The morphodynamics of the Scheldt estuary is the result of the natural sediment transport but also the anthropogenic activities such as channel deepening, sand mining, and channel dredging (Elias et al., 2023). The natural sediment transport in the Scheldt has been shown to result from tidal asymmetry (Wang et al., 2002). Tidal asymmetry is the variation in propagation speed of the tidal wave crest (flood) and trough (ebb). Medium and long-term morphodynamic modeling models have demonstrated its effect using morphodynamic numerical models (Bolle et al., 2010; Dam et al., 2016). On the other hand, the anthropogenic effects on the morphodynamics have been investigated by van der Wegen & Roelvink (2012). This model identified specific dredging and dumping areas along the estuary.

Some morphodynamic modeling of the Scheldt estuary used Delft3D. The work by Van Der Wegen & Roelvink (2008) did not include the mud content and applied sand transport formulas (van Rijn, 2007a) for the sand fractions found along the channel. The research by Elmilady et al. (2022) investigated the effect of sea level rise on the morphodynamics of a constrained system similar to the Western Scheldt.

Wadden sea

According to the classification of Bosboom & Stive (2021), the Wadden sea is a barrier and lagoon coast that is dominated by both tides and waves, depending on its location. It spans 500 km along the North Sea coasts of The Netherlands, Germany, and Denmark. It is the world's largest uninterrupted system of barrier islands and tidal flats. Because of the ecological value of the intertidal zones, efforts have been made to collect data to support the management of this system. One such project is the Synoptic Intertidal Benthic Survey (SIBES) that covers the entire Dutch and part of the German Wadden Sea. This data set contains annually sampled data in the Dutch intertidal area from 7,400 locations since 2008, while the rest of the Dutch subtidal and German Wadden Sea have only been sampled once. A spatial data model of the bed level and percentage of mud are show in Figure 4.

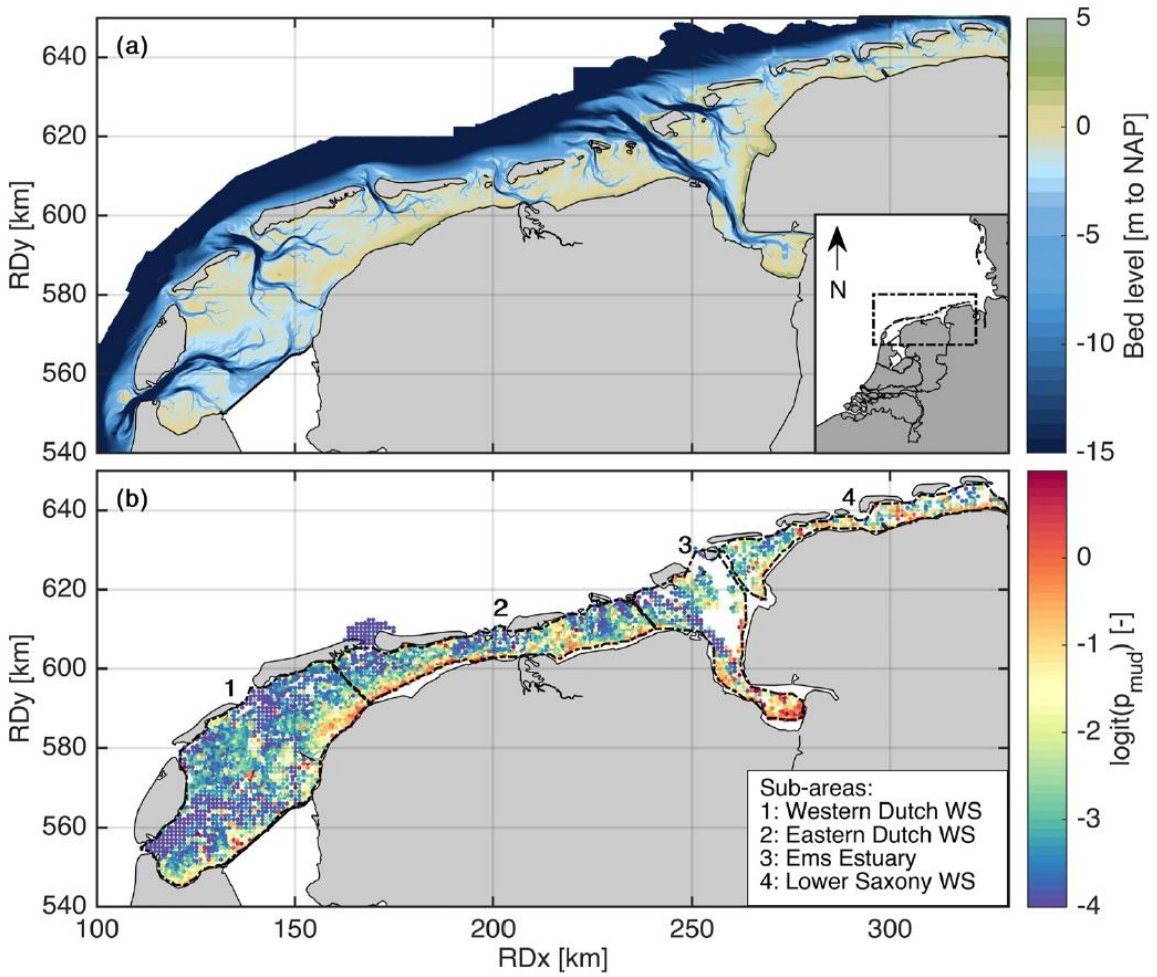

Figure 4. Wadden Sea model (from Western Dutch Wadden Sea to Lower Saxony Wadden Sea) showing bathymetry (top) and percentage of mud (bottom) between 2009-2018 (Colina Alonso et al., 2022).

Morphodynamic modeling of this system has been confined to the modeling of a single inlet. Attempting to model the entire system would require significant computational resources. Alternatively, Dissanayake et al. (2009) recommended the Ameland inlet due to its minimal connectivity to adjacent basins rendering it almost closed. Colina Alonso et al. (2023) implemented the modified version of the sand-mud transport equations of van Ledden (2002) into Delft3D to investigate the role of sand-mud in morphodynamics. Dissanayake et al. (2009) also used Delft3D to study the effect of different sea level rise scenarios on basin morphodynamics.

Yangtze river

The Yangtze river estuary is one of the largest estuaries in the world (Zhao et al., 2023) with the width of the estuary increasing from 6 km to 9 km at the mouth. Figure 5 shows a bathymetry of the Yangtze river estuary (Feng et al., 2020). The suspended sediments are mostly composed of fine sediments (i.e. clays and silts) and there exists an estuary turbidity maximum (ETM) at the mouth of the estuary. This ETM varies in area depending on the season or tide (Zhao et al., 2023). Recent literature on the Yangtze have focused on understanding the morphological changes brought about by the construction of the Three Gorges Dam (Kuang et al., 2013; Luo et al., 2022; Zhao et al., 2023), and the effects of climate change either from increased river discharge (Kuang et al., 2017) or sea level rise (Chen et al., 2024; Kuang et al., 2017).

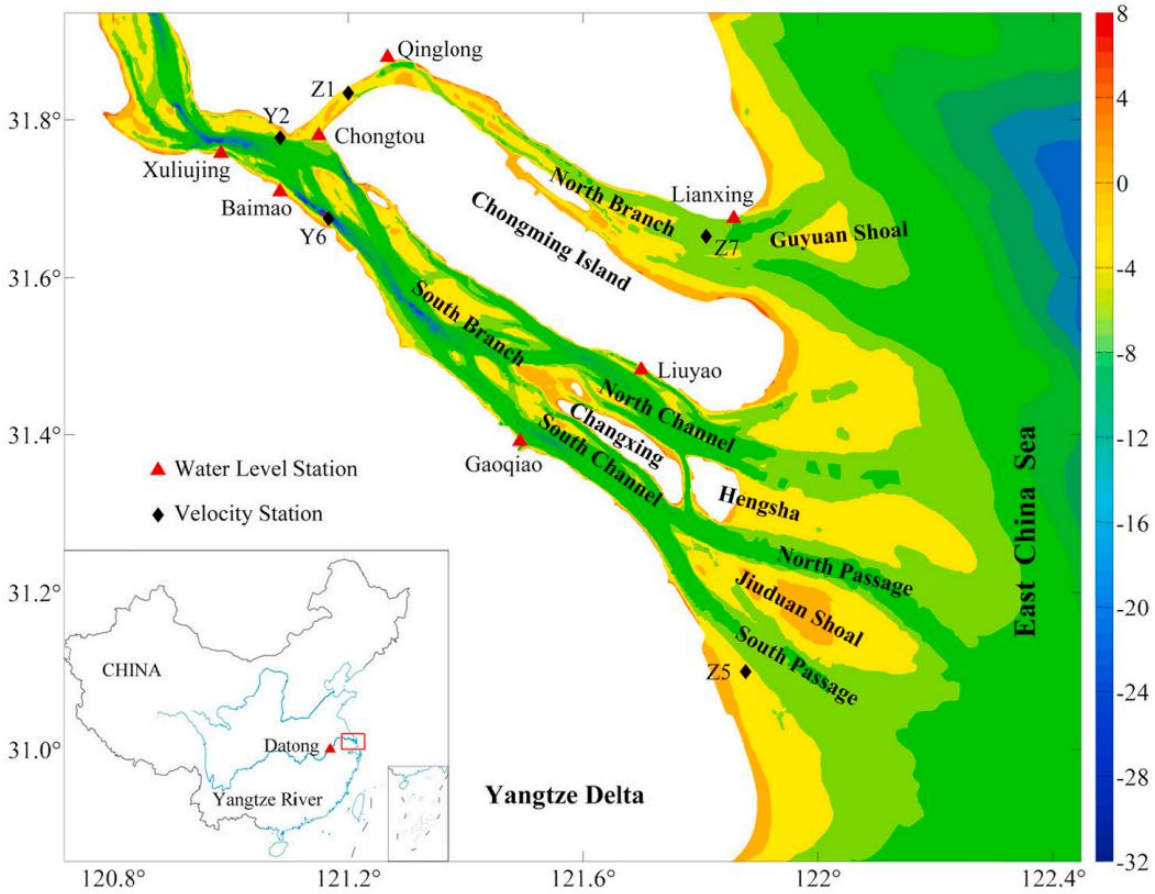

Figure 5. Bathymetry map of the Yangtze river estuaries with markers for water level and velocity measurement stations (Feng et al., 2020)

Morphodynamic modeling and the near-bed exchange process was modeled by Delft3D. Zhu et al. (2021) explored the mechanisms of the ETM from either a sediment- or salinity-induced density gradient. Guo et al. (2015) also used Delft3D to explore the role of river discharge on the morphology of schematized version of the estuary. Finally, Kuang et al. (2017) created morphodynamic models to simulate the effect of climate change to the system. For the Yangtze, climate change can either come in the form of increased river discharge and/or sea level rise. Other sea level rise studies used different morphodynamic models, such as DHI Mike (Chen et al., 2024).

Mekong river delta

The Mekong river delta is the end point of a transboundary river that runs through China, Myanmar, Thailand, Laos, Cambodia, and Vietnam. The bathymetry of the delta is shown in Figure 6. Wang et al. (2024) took 134 surface sediment samples within the delta and characterizes the bed as sand-mud with some locations containing gravel. Unverricht et al. (2013) tooks samples at the subaqueous region of the Mekong delta and found sediment to be mostly different proportions of sand-silt.

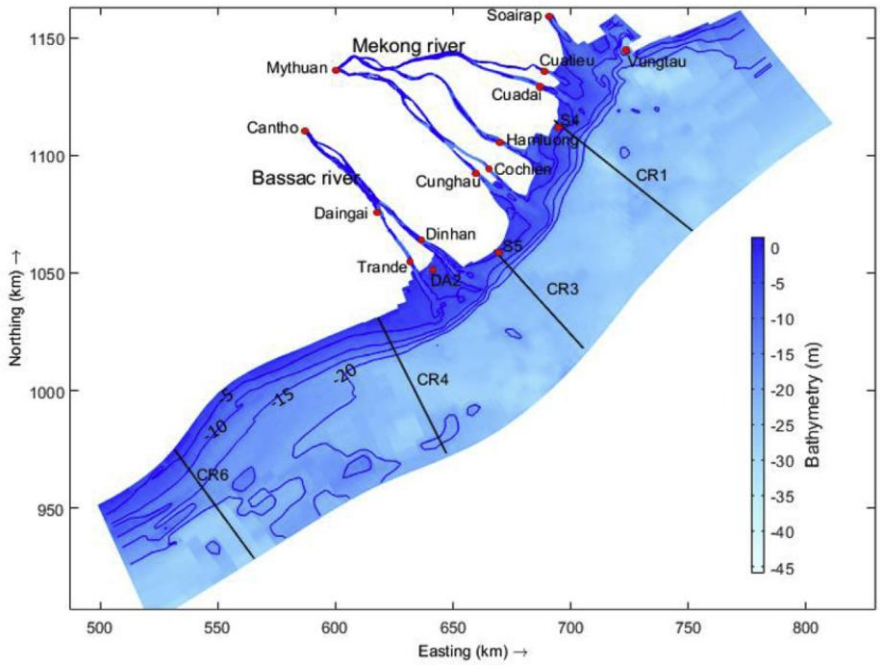

Figure 6. Bathymetry model of Mekong river delta (Tu et al., 2019). The figure also reflect cities along the Mekong river and cross-shore transects used to calculate cumulative longshore sediment transport.

The modeling work on the Mekong delta used multiple models such as Delft3D or another model called the SCS 3D circulation model. The Delft3D model in Tu et al. (2019) investigated the changes to sediment transport and morphodynamics of the system by applying different impact drivers. These impact drivers consisted of reduced upstream sediment supply from upstream dam construction and sand mining along the river. Wang et al. (2024) investigated sediment transport due to ocean currents driven by the East Asian monsoons.

2.3. COMPARATIVE STUDIES OF DIFFERENT SAND-MUD SYSTEMS

Research on estuaries such as those presented in the previous section are typically done by research institutions close to the location of the estuaries. Comparative analyses between different estuarine systems are rare, and because of this, theories and studies that describe morphodynamics of a system are tailored to that system. The following comparative studies show a progression in the analysis of estuaries around the world.

Galloway (1975) studied the morphological change in delta progradation based on the change in dominant hydrodynamics across geological time scales. The study quantified the changes in plan form and stratigraphy in terms of the intensity of different deltaic processes (i.e. tide-, wave-, fluvial-dominant systems). This work demonstrates a methodology to classify estuaries but is on a timescale not compatible with the RANS morphodynamic models.

A global analysis of delta morphology based on hydrologic data was done by Nienhuis et al. (2020). Figure 7 shows the deltas around the world that were included in this study together with the dominant hydrodynamics of each delta. The study calculated the delta's area loss or gain by considering the sediment flux from different sources (e.g. tide, wave, fluvial) using an empirical equation. The study provided a first order estimate of delta area change but does not consider the sediment characteristics, i.e. sand/silt/clay. The study then compared their results to vectorized worldwide shoreline datasets to demonstrate the accuracy of using an empirical equation. The method resulted in an 85% accuracy in predicting delta morphology.

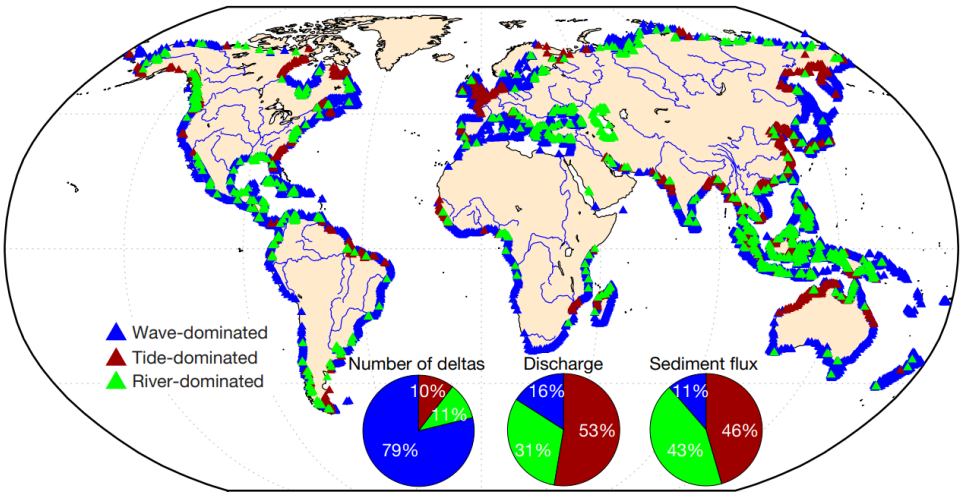

Figure 7. Deltas and their dominant hydrodynamics around the world (Nienhuis et al., 2020) The pie charts in the figure reflect what percentage of the world's deltas are dominated by different hydrodynamic processes (i.e. wave-, tide-, river-dominate. Also in the figure is how much each hydrodynamic process contributes to the total discharge and sediment flux in deltas.

More recently, the work by Jiang et al. (2024) investigated the impacts of sediment composition on long-term estuarine and deltaic morphodynamics. The study used Delft3D and simulated the morphodynamics using an idealized model. Figure 8 shows the morphodynamic evolution results of 2 simulations with different sand-mud ratios run for 200 years. The hydrodynamics used in the model were based on the information from the Yangtze river. The sediment erosion parameters used were not specific to sediment composition but taken from existing literature and based on sensitivity analyses. The study found that the content of cohesive sediment in estuarine beds was a good indicator of the speed of morphodynamic estuarine development. Further, the study highlighted the importance of realistic representations of bed compositions in the long-term morphodynamic modeling of estuaries.

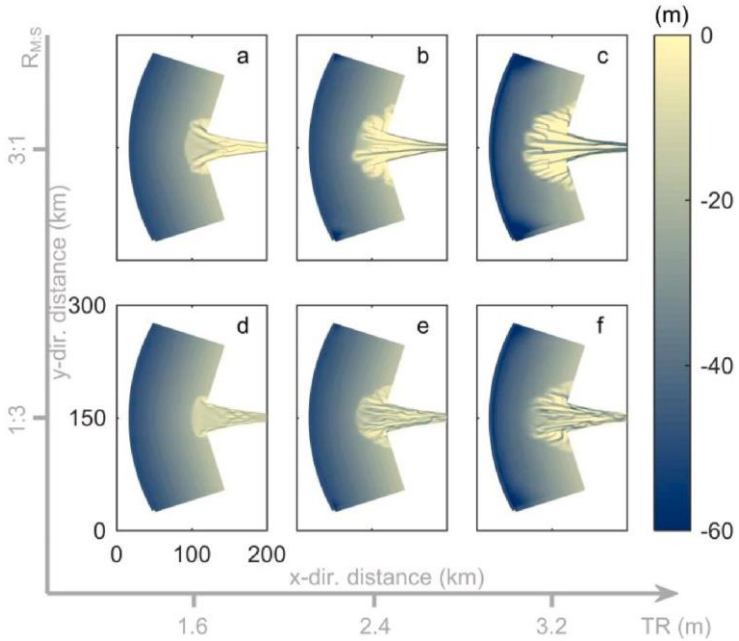

Figure 8. Morphodynamic evolution of idealized estuary with different sand-mud ratios (Jiang et al., 2024) after 200 years. Subfigures a to c used a mud-sand ratio of 3:1 while subfigures d to f used mud-sand ratio of 1:3.

3. PHYSICAL PROCESSES AND MATHEMATICAL MODELS IN SAND-MUD TRANSPORT

To understand the mechanisms behind sand-mud dynamics, transport processes are discussed in the following section. Additionally, the current mathematical models used to quantify each process are also presented.

3.1. BOUNDARY LAYER HYDRODYNAMICS

Open channel flow in the real world is generally characterized as turbulent. Turbulence produces shear that is quantified using the Boussinesq approximation shown in Eq. 1. This relationship introduces the eddy viscosity term that models turbulent diffusion similar to molecular diffusion. Turbulent diffusion occurs at higher speeds which results in more efficient mixing in the water column.

$$\tau_{xz} = -\rho\overline{u'w'} \equiv \rho\nu_T \frac{du}{dz} \quad (1)$$

where, τ_{xz} – Reynolds stress, ρ – fluid density, $\overline{u'w'}$ – turbulent shear, ν_T – eddy viscosity.
From experiments, Prandtl describes the velocity profile at the boundary layer as logarithmic. This description assumes a turbulent mixing length that scales with distance from the bed and a friction velocity defined by the bed shear stress and the fluid density. The logarithmic profile is known as the law of the wall and is presented in Eq. 2.

$$u = \frac{u_*}{\kappa} \ln\left(\frac{z}{z_0}\right) \quad (2)$$

where, u – velocity, $u_* \equiv \sqrt{\tau_b/\rho}$ - shear velocity, τ_b – bed shear stress, $\kappa = 0.41$ – Von Karman constant, z – depth from bed, z_0 – roughness length.

However, in real world systems, the density of the fluid is not uniform. This is a result of differences in temperature, salinity and sediment concentration. Estuaries are particularly subject to non-uniform density from salinity and sediment concentration gradients. Turbulence plays a role in mixing these quantities across the water column. In terms of sediment transport, turbulence provides the energy to lift sediment particles from the boundary layer to the upper portions of the water column (Figure 9).

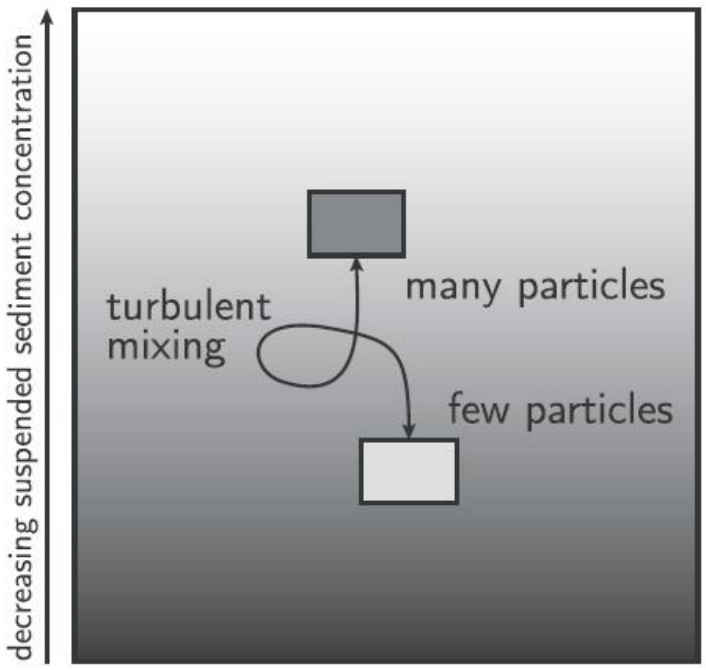

Figure 9. Sketch of particle advection due to turbulent mixing (Winterwerp et al., 2021)

Bed shear stress results from the logarithmic velocity profile near the bed. It is the main producer of turbulence near the bed and is key in fine sediment analysis (Winterwerp et al., 2021). Bed shear stress is typically calculated as a function of fluid density, a characteristic velocity, and a frictional coefficient as shown in Eq. 3.

$$\tau_b = c_f U^2 \rho \quad (3)$$

where, c_f – frictional coefficient, U – characteristic velocity.

In terms of momentum, the frictional coefficients describes the total energy loss of a moving fluid or the total hydraulic drag. Total hydraulic drag is the combined drag from the skin drag and form drag. Skin drag is the energy loss of the moving fluid from the individual sediment particles that make up the bed. Form drag is the energy loss from all other sources such as bed forms (i.e. ripples). From this distinction, it is the skin friction that erodes sediment from the bed. It is this framework that introduced the concept of a critical shear stress.

3.2. CRITICAL SHEAR STRESS AND EROSION

The critical shear stress is the stress necessary for the incipient motion of a single sediment particle to take place. Shields (1936) introduced a parameter, now called the critical Shields parameter, that describes incipient motion and relates the shear stress acting on an individual sediment particle with its apparent weight (Eq. 4). Shields analyzed this parameter across different flow regimes.

$$\theta_{cr} = \frac{\tau_{b,cr}}{(\rho_s - \rho) g d_{50}} \quad (4)$$

where, θ – Shields parameter, $\tau_{b,cr}$ – critical bed shear stress, ρ_s – density of sediment, d_{50} – typically median diameter.

Incipient motion is not straightforward in the sand-mud environments. Sand-mud erodes in different modes: particle, surface, and mass erosion (van Rijn, 2020; Winterwerp et al., 2021). These modes have not been differentiated quantitatively but made distinct through observation. Particle erosion is the erosion of the sediment surface in minor clouds of fines. Surface erosion is observed when small craters appear on the bed surface. Finally, mass erosion is observed when there local failure of the bed coupled with large clouds of mud. Thus, determining which erosion mode is observed during experiments is a highly subjective endeavor. Van Prooijen & Winterwerp (2010) and Jacobs et al. (2011) have suggested defining critical bed shear stress as a point between the range of particle and surface erosion shear stress values.

Aside from the subjectivity of determining erosion modes, different mechanisms act on sand-mud beds. Different quantities of each sediment fraction results in various degrees of contribution from each mechanism. The mass fraction of clay particles is used to determine whether a sand-mud bed is cohesive or not (Van Ledden et al., 2004; Winterwerp & van Kesteren, 2004). The resulting network structure of sediment particles also has an effect on the strength of sand-mud beds. Van Ledden et al. (2004) and Jacobs (2011) have discussed network structures and its effect on bed strength. Together, cohesion from clay particles and the resulting network of sediments makes determining the critical shear stress for sand-mud sediments difficult.

Research like that of Mehta (1988), Mitchener et al. (1997), Roberts et al. (1998), van Rijn (2007b), Wu et al. (2018), and Yao et al. (2022) have attempted to describe incipient motion across a range of sediment sizes and other sand-mud properties such as bulk density. Reanalysis of the data these studies used must be done with care as not all of them determined critical shear stress in the same manner. No consensus has been reached concerning the most appropriate method of calculating critical shear stress for all types of sand-mud beds. What is clear from all the descriptions of incipient motion is that the presence of cohesive sediments increases the critical shear stress.

Different researchers have treated this differently. As an example, van Rijn (2007a) added a factor that increases with increasing mud content (Eq. 5).

$$\tau_{b,cr} = \begin{cases} (\rho_s - \rho) g d_{50} \theta_{cr} \left(1 + p_{clay}\right)^3 & \text{for} \quad d_{50} \geq 62\ \mu m \\ (\rho_s - \rho) g d_{50} \theta_{cr} \left(\phi_s / \phi_{s,max,sand}\right) (d_{sand}/d_{50})^{\gamma} & \text{for} \quad d_{50} < 62\ \mu m \end{cases} \qquad 5$$

where, p_{mud} – percentage of mud in sediment sample, ϕ_s – solid fraction, $\phi_{s,max,sand}$ – maximum solid fraction for sand $= 0.65$, γ – exponent between 1 and 2.

Of note are the works by te Slaa (2020) and Yao et al. (2022) who investigated the erosion process of silt. te Slaa (2020) modeled erosion using the a version of van Rijn (2007a) (Eq. 5).

Yao et al. (2022) describes different mechanisms of erosion compared with the other work that collectively described clay and silt as mud. The result of Yao's work is similar to van Rijn's in that there is a factor that increases critical shear stress if the mass fraction of silt exceeds 35%.

$$\tau_{b,cr} = (\rho_s - \rho) g d_{50} \theta_{cr} (1 + \beta_{ss}) \qquad 6$$

where, β_{ss} – parameter representing effects of Silt-Structural force $= \frac{\alpha_{Yao}}{(s-1) g {d_{50}}^2}$, s – relative density of sediment grains $= \rho_s/\rho$, α_{Yao} – expanded cohesive parameter $= 5.2 \times 10^{-8}\ \mathrm{m^3/s^2}$.

A continuous application of shear stress on the bed will result in the transport of sediments and erosion. After enough particles have been eroded and transported the bed level will change. The transport of sand and mud are different. Sand or non-cohesive transport is determined by the flow capacity of the fluid. Hence, the erosion is described as the volume of transported sediment. Present day models of non-cohesive sediment transport follow the form of Meyer-Peter & Müller (1948). A limitation of this initial description is that this only quantifies the transport of sediments along the bed, or bedload transport.

On the other hand, mud transport is supply limited. This means that volume of transported mud is not a function of the flow but controlled by the amount of sediment eroded. The mathematical formula for erosion is based on the equation of Partheniades (1965) for cohesive soils. This formula describes the erosion of cohesive sediment beds based on excess bed shear stress, $(\tau_b - \tau_{cr})$ or nondimensionally $(\tau_b/\tau_{cr} - 1)$, and an erosion parameter, M, for mud beds. The transport process is also unlike non-cohesive sediment in that cohesive sediment is transported only by suspended load.

The erosion parameter, M, is not the subject of a lot of research despite its direct effect on the erosion rate of sand-mud beds. Jacobs (2011) presents literature on the erosion parameter for cohesive sediments while te Slaa (2020) derived a new formulation for the erosion parameter of silt.

The differences in mechanisms of erosion between non-cohesive and cohesive sediments make erosion estimation for sand-mud difficult. One example is the erosion rate formulas of Van Ledden (2003). The erosion formula are based on the difference in erosion behavior for non-cohesive and cohesive beds. Van Ledden proposes a critical mud content. If the bed mud content is higher, then the erosion behavior of the bed is similar to a cohesive bed. However, if the bed mud content is lower than the critical mud content, then the bed behaves like a non-cohesive bed. Colina Alonso et al. (2023) provides a schematic diagram in Figure 10 of sand-mud beds illustrating the differences between cohesive and non-cohesive beds. Torfs (1995) argues that estimating the erosion rate for sand/non-cohesive sediment for low mud content can use sand transport formulas like van Rijn (1993) and shown in Eq. 7. The erosion rate equations for mud in low mud environments, and sand and mud in higher mud environments are presented in Eq. 8, Eq. 9 and Eq. 10.

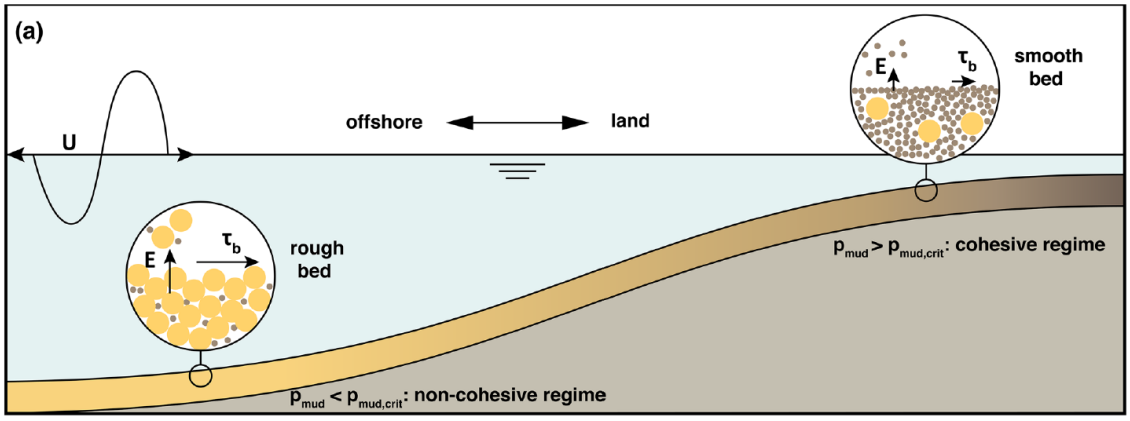

Figure 10. Schematic diagram of different types of sand-mud beds (Colina Alonso et al., 2023). Mud fraction less than a determined critical mud content classifies a sand-mud bed in the non-cohesive regime while mud fraction greater than the critical mud content is a bed in the cohesive regime.

$$E_{s,nc} = \frac{\alpha_{b1}}{3}\frac{\sqrt{\Delta g d_{50}}}{{D_*}^{0.9}}{T_{nc}}^{\alpha_{b2}-0.9} \quad 7$$

$$E_{m,nc} = \frac{p_m}{1-p_m}\frac{\alpha_{b1}}{3}\frac{\sqrt{\Delta g d_{50}}}{{D_*}^{0.9}}{T_{nc}}^{\alpha_{b2}-0.9} \quad 8$$

$$E_{s,c} = (1-p_m)M_c\left(\frac{\tau_b}{\tau_{b,cr,c}}-1\right)H\left(\frac{\tau_b}{\tau_{b,cr,c}}-1\right) \quad 9$$

$$E_{m,c} = p_m M_c\left(\frac{\tau_b}{\tau_{b,cr,c}}-1\right)H\left(\frac{\tau_b}{\tau_{b,cr,c}}-1\right) \quad 10$$

where, $E_{m,nc}$ – erosion rate of mud for non-cohesive sediment mixture, $E_{m,c}$ – erosion rate of mud for cohesive sediment mixture, $E_{s,c}$ – erosion rate of sand for cohesive sediment mixture, T_{nc} – transport parameter $= \frac{\tau_b}{\tau_{b,cr,nc}(1+p_{mud})^{\beta}} - 1$, $\tau_{b,cr,nc}$ – critical shear stress of non-cohesive sediment, β parameter between 0.75 to 1.25, $\alpha_{b1} = 0.053$ for $T < 3$ and $= 0.1$ $T > 3$, $\alpha_{b2} = 2.1$ for $T < 3$ and$=$ 1.5 $T > 3$, $D_* = d_{50}\sqrt[3]{\frac{\Delta g}{\nu^2}}$ – dimensionless diameter, M_c – erosion parameter for cohesive sand-mud mixtures, $\tau_{b,cr,c}$ – critical shear stress of cohesive sediment, H is the Heaviside function which is 1 when the function is > 0 and 0 when the function is ≤ 0.

At present, the research done on critical shear stress and erosion of sand-mud lumps silt and clay into the mud parameter. No correction or factors has been added to the current formulations to account for the different silt/clay content in sand-mud sediment environments.

3.3. FLOCCULATION AND HINDERED SETTLING

Once suspended, the cohesion binds cohesive sediments into what is known as a floc. The process of this binding is called flocculation and is only present when cohesive sediments are involved. Flocs, its properties, and the process of flocculation have been extensively studied (Cuthbertson et al., 2018; Manning et al., 2010, 2011; Mikeš & Manning, 2010; Schwarz et al., 2017; van Rijn & Barth, 2019; Winterwerp, 1998; Winterwerp et al., 2006; Xu et al., 2022). Unlike in non-cohesive sediment where the settling of sediment particles is governed and fixed by the individual particle's physical properties, the settling of mixed sediments as flocs is dependent on size and openness of the floc. Openness here is used to describe the amount of space between individual particles in a single floc. This dependence on multiple, time-dependent properties makes it difficult to ascertain a representative settling velocity of sand-mud sediments.

Due to the network structure of floc, flocs are described by their a parameter called gelling concentration. The gelling concentration or c_{gel} is the mass concentration when flocs form a space-

filling network. This concentration depends on the openness of the flocs. A more open floc has less mass when occupying the same volume compared with a less open floc. Therefore, more open flocs result in a lower gelling concentration than less open flocs.

As suspended sediment concentration increases, hindered settling is observed. Winterwerp et al. (2021) presents a proposed equation for hindered settling that is a function of sediment solid fraction and volumetric floc concentration (Eq. 11).

$$w_s = w_{s,0} \frac{(1-\phi_f)^2 (1-\phi_s)}{1+2.5\phi_f} \qquad 11$$

Where w_s – hindered settling velocity, $w_{s,0}$ – settling velocity of a single floc in still water, $\phi_f = c/c_{gel}$ – floc concentration, ϕ_f – sediment solid fraction.

Figure 11 illustrates data points from experiments showing both the settling and hindered settling regimes as a function of suspended particulate matter (SPM) concentration and gelling concentrations (Winterwerp et al., 2021). For lower SPM concentrations, the relationship is linear. At higher concentrations, fluid flow between particles is strained and start to act on the settling particles thereby exhibiting hindered settling. The trend lines in the hindered settling regime are from Eq. 11.

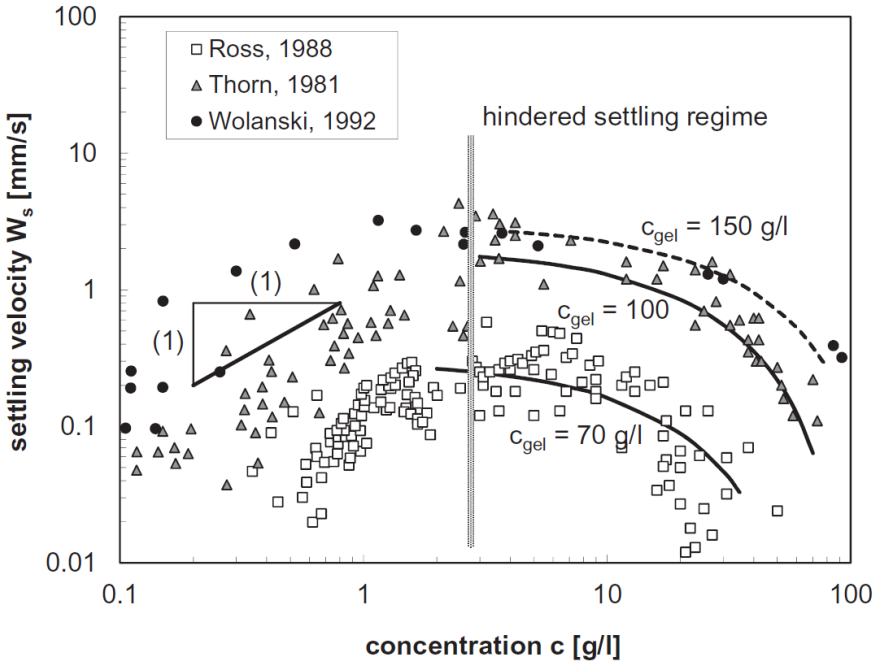

Figure 11. Settling velocity and hindered settling regimes as a function of suspended particulate matter (SPM) (Winterwerp et al., 2021)

3.4. DEPOSITION AND CONSOLIDATION

The process of deposition is a direct result of the settling of suspended particles. Larger and heavier particles, like sand, settle first and are not much affected by the longer timescales from hindered settling. This results in a segregated bed with heavier particles below the lighter smaller particles. te Slaa (2020) shows a time series of deposition in terms of measured solid content in Figure 12. The red points on the graph are measured solid concentration and the rainbow color spectrum shows the evolution of depositing solid content of the sediment.

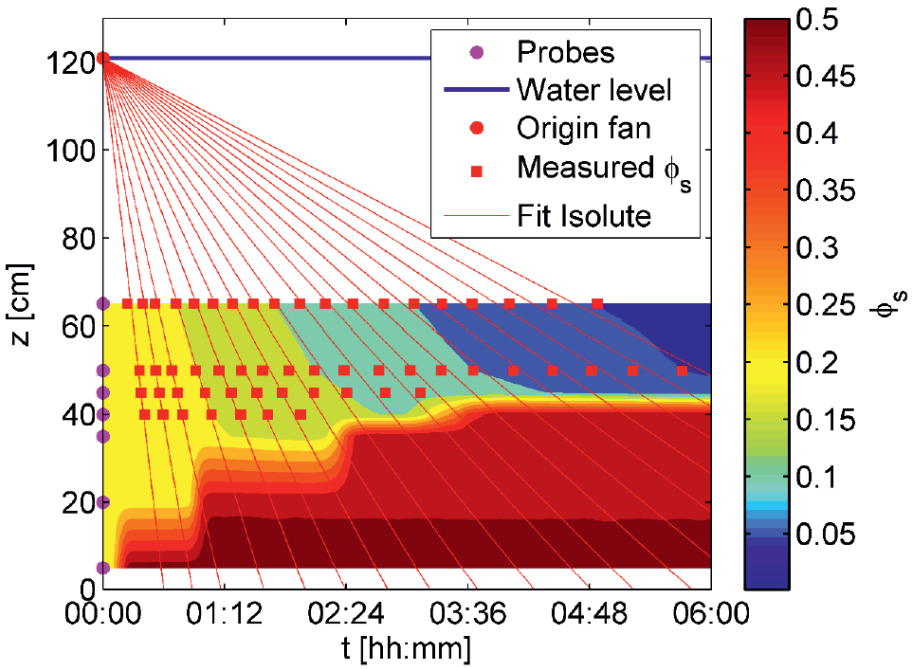

Figure 12. Time series of hindered settling in terms of measured solid concentration (te Slaa, 2020)

Deposition of sand-mud sediments can be modeled in numerical simulations using the formula called reduced deposition shown in Eq 12 which is based on the deposition equation for cohesive sediment (Einstein & Krone, 1962). Here the deposition is a function of settling velocity, and the near-bed suspended particulate matter concentration, as well as a factor to parameterize the other unresolved processes (Winterwerp et al., 2021). These parameterized processes include hindered settling, floc break-up, strength development of deposited flocs, resolution of numerical simulations, sediment balance of numerical simulations.

$$D = p_d w_{s,b} c_b \qquad 12$$

where D – deposition rate, $w_{s,b}$ – near-bed settling velocity, c_b – near-bed SPM concentration, p_d – reduced deposition coefficient.

As the suspended particles reach the bed, a point referred to as the point of contraction is reached where the water-sediment interface coincides with the level whose solid concentration equals the gelling concentration. After such a point, the individual particles rearrange themselves from the overburden pressure of lighter sediments. Figure 13 sketches the water-sediment interface as the particles transition from hindered settling phase to consolidation phase (Winterwerp et al., 2021). During the consolidation phase, water trapped between the clay particles is slowly expelled thereby lowering the interface further.

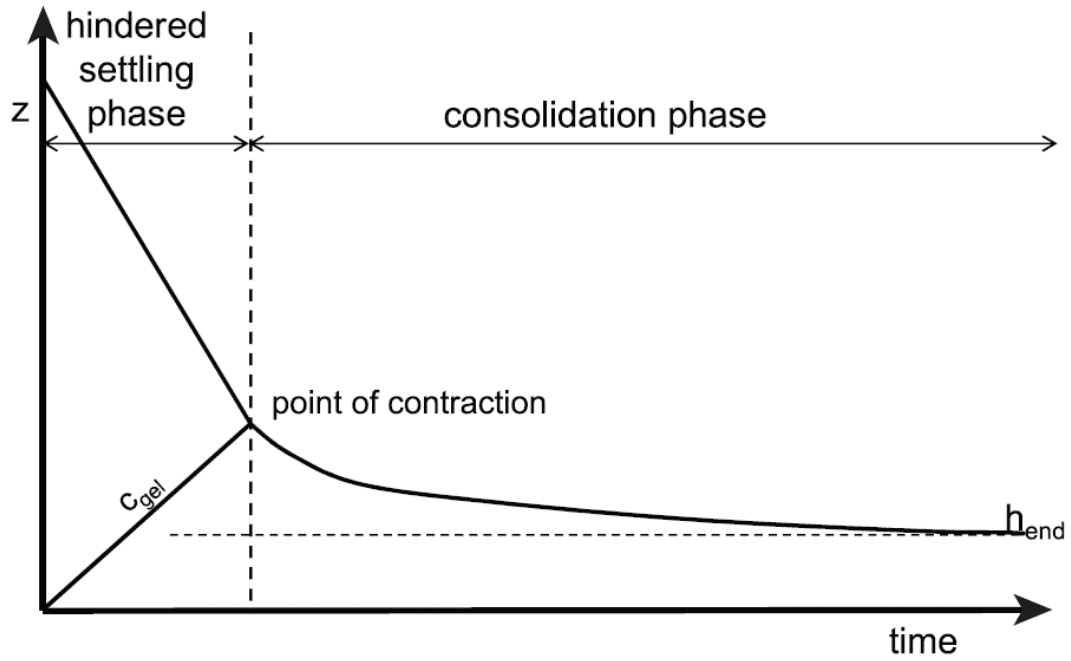

Figure 13. Water-sediment interface evolution from hindered settling to consolidation phase (Winterwerp et al., 2021)

It can be observed that the interface settles rapidly during the hindered settling phase but approaches the final elevation asymptotically. This prolonged consolidation can be attributed to the very small hydraulic conductivity of the fines (e.g. silt and clay). Typical time scales for hindered settling is in the order of minutes while for equilibrium condition of consolidation is in the order of weeks (Winterwerp et al., 2021).

Consolidation of sand-mud beds have not been studied extensively. Flume experiments are unable to replicate the time-varying strength development of a consolidated beds because of the time scales involved. Most flume experiment allow for some consolidation for 24 hours after artificially mixing different sediment classes. However, this time is insufficient to replicate naturally consolidated beds. On the other hand, it is difficult to collect undisturbed samples of consolidated beds for flume experiments.

Current models for consolidation of beds are based on site-specific datasets. The work by Allersma (1988) provides an empirical relationship between the dry volume of sand and the dry density of sand-mud. The equation has an additional parameter, α_c, to account for consolidation and has recommended values for freshly deposited (0) to old deposited sediment (2.4).

More recently, the work by Van Rijn et al., 2025 proposed a relationship between the dry bulk density and the sediment classes of sand-mud for data from the Dutch Wadden Sea at the end of primary consolidation. This equation also has a factor, f_c, to account for consolidation. This factor also has recommended value for freshly deposited (0.5) to old deposited sediment (1.0)

4. HYDRO-MORPHODYNAMIC RANS MODELS OF SAND-MUD: DELFT3D 4 OR DELFT3D FM

4.1. HYDRODYNAMIC SCHEME

Delft3D solves the non-linear shallow water equations in two (depth-averaged) or in three dimensions. These equations are derived from the 3D Navier-Stokes equations for incompressible free surface flow (Deltares, 2023).

The turbulent processes are incorporated in a sub-grid using space- and time-averaged quantities. Delft3D supports the following turbulence closure models:

1. Constant coefficient
2. Algebraic eddy viscosity closure model
3. $k - L$ turbulence closure model
4. $k - \varepsilon$ turbulence closure model

The hydrodynamic formulation use a finite different scheme for Delft3D 4 and a finite element method scheme for Delft3D FM. Modeling on Delft3D 4 is based on a structured grid while Delft3D FM is modeled on an unstructured grid. Delft3D FM allows for extra flexibility in grid modeling because multiple grid shapes are possible.

In relation to morphodynamics, the boundary layer hydrodynamics are also solved. The bed shear stress is calculated using a modified version of the law of the wall. This modification takes into account the discretization of the vertical layers.

4.2. MORPHODYNAMIC MODELING

Delft3D allows for the schematization of suspended and bedload. Suspended load can be further schematized into mud and sand or cohesive and non-cohesive fractions, respectively. These fractions have pre-defined characteristics and Delft3D allows for up to 99 different sand or mud fractions. The bedload is non-cohesive transport and is estimated using one of the multiple equations encoded into Delft3D (Deltares, 2023).

The morphological update scheme is presented in a schematic diagram in Figure 14. From the initial and boundary conditions, hydrodynamics are solved first followed by the sediment transport rates. A morphological factor, MorFac, is included before updating bed levels. The scheme closes the loop by resolving the hydrodynamics after updating bed levels.

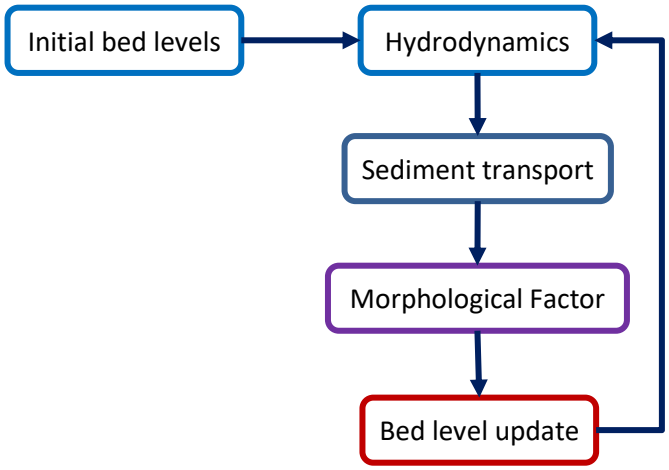

Figure 14. Morphological update scheme of Delft3D (Van Der Wegen & Roelvink, 2008)

Van Der Wegen & Roelvink (2008) discusses that, for tide-dominated estuaries, hydrodynamic behavior is at a different timescale to morphodynamic timescales. Significant change in morphodynamics is only seen after several hydrodynamic calculations. The MorFac increases the bed level change to "speed up" the effect of the morphodynamics. It should be noted that using MorFac is only valid for when bed level changes remain small compared to water depth after 1 time step.

The fluff layer module creates a separate mud fraction on the top most bed layer. The layer is named as such because it contains the freshly deposited mud. This type of mud has lower strength compared to more consolidated mud, and is easily eroded. The erosion rate of the fluff layer is dependent on the amount of sediment in this layer. A reduced erosion rate is calculated based on a user-defined ratio, M_0/M_1. M_0 $(kg/m^2/s)$ is a zero-order erosion parameter or the erosion parameter M in the Partheniades erosion equation, and $M_1(1/s)$ is the first-order erosion parameter for limited sediment availability. If the mass of sediment per unit area in the fluff layer is less than M_0/M_1, the erosion rate in the fluff layer is linearly reduced as shown in Eq 13. This reduced erosion rate displays a more realistic model behavior for sand-mud environments. Conversely, if the mass of sediment per unit area exceeds the ratio, the erosion rate reverts back to the Partheniades erosion formula. The erosion rate of the bed is similar to Eq. 10.

$$E_{fluff} = \begin{cases} mM_1\left(\dfrac{\tau}{\tau_{cr,f}} - 1\right) & : \quad m < \dfrac{M_0}{M_1} \\ M_0\left(\dfrac{\tau}{\tau_{cr,f}} - 1\right) & : \quad m > \dfrac{M_0}{M_1} \end{cases} \qquad 13$$

4.3. EXAMPLE CASES OF SAND-MUD MORPHODYNAMIC MODELING

After a brief overview of the morphodynamic scheme in Delft3D 4 or FM, let us look at some literature that made use of this scheme. The examples give different aspects of morphodynamic modeling. Some used idealized domains while others made use of real world estuaries and different ways to describe the sediment classes and near-bed erosion behavior.

van Maren et al. (2009) modeled hyperconcentrated flows in the Yellow river using a schematized domain. Hydrodynamic parameters in the model were taken from the measured flow conditions. On the other hand, morphodynamic parameters sought the appropriate erosion rate rather than identifying the exact value for critical bed shear stress. Therefore, the erosion parameter, M, was used to calibrate the erosion rate while the critical bed shear stress values were fixed at 1 Pa. Figure 15 shows cross-sectional bed level changes for different M values. From their methodology, the realistic value for erosion parameter, M, is at 5.0 x 10^{-4} kg/m^2/s.

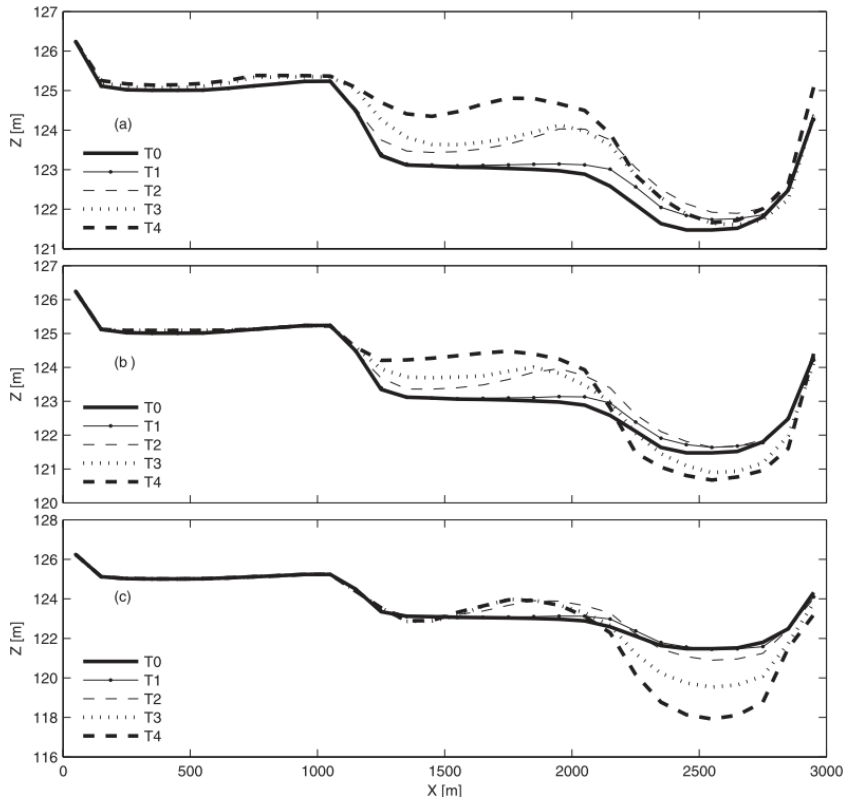

Figure 15. Cross-sectional bed level evolution using different M parameters (van Maren et al., 2009)

van Maren et al. (2020) studied the observed coastal turbidity maximum near the Zeebrugge harbor and the mouth of the Scheldt estuary. The sediment characteristics were based on previous numerical modeling work done in the southern North Sea. The study also identified literature that describe a fluffy layer near the seabed that is made up of freshly deposited mud. Because of the presence of this fluff layer, the modeling done for this study utilized the fluff layer module of Delft3D.

The study site presented 2 types of mud: mud deposited at the bed due to transport and consolidated mud from a Holocene mud deposit at the mouth of the Scheldt estuary. The investigation looked into the morphodynamics resulting from the transport of fluffy mud and the erosion and transport of the Holocene mud. The critical bed shear stress of both sand and mud were kept constant and variation in the erosion of either sediment fraction is based on the erosion parameter, M. Figure 16 shows the resulting surface suspended sediment concentration when factoring in mud contributions from the fluff and the Holocene deposit.

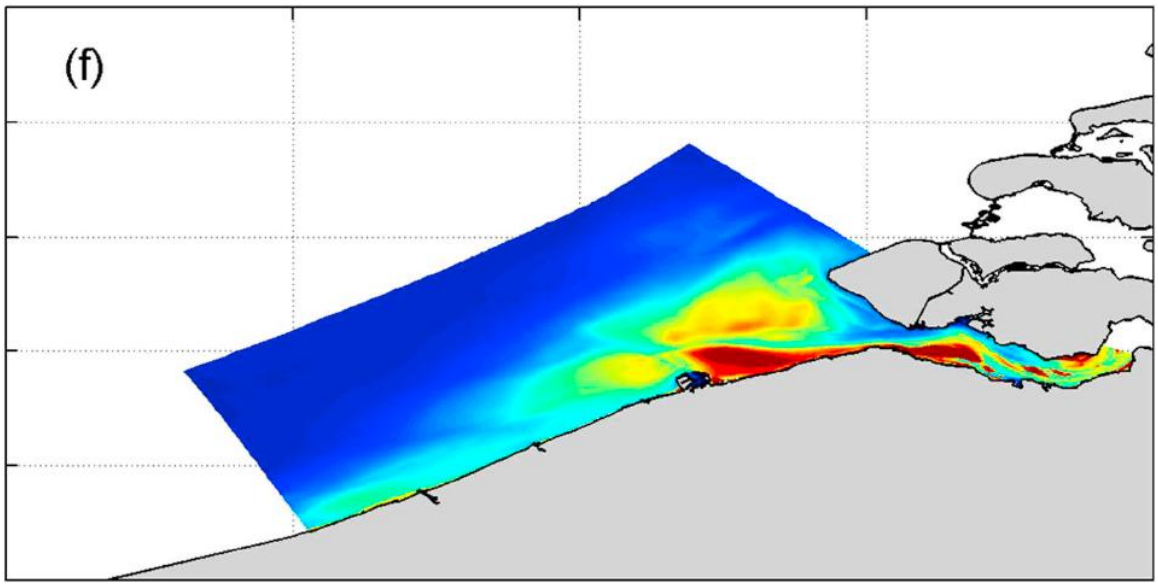

Figure 16. Model results for surface suspended sediment concentration (van Maren et al., 2020)

Colina Alonso et al. (2023) analyzed the role of sand-mud interaction in the morphodynamic modeling of a schematized version of 1 tidal basin in the Wadden Sea. The Delft3D model was forced using semi-diurnal tidal amplitudes from the North sea and used a spin-up period of 50 years. The bathymetry was initially sloped with uniform sediment composition. The bed consisted of 1 sand and 1 mud fraction. Finally, this simulation used a MorFac of 50.

This version of Delft3D used spatially-varying values for critical bed shear stress based on the mass fraction of mud. Figure 17 shows the resulting morphodynamics and bed composition of simulations with and without sand-mud interaction. This implementation was an updated version to the work proposed by Van Ledden (2003) that solves for the erosion rate of mud based on the mass fraction of mud. Their results demonstrated the need to account for sand-mud interaction to improve the predictive ability of tidal basin evolution numerical models.

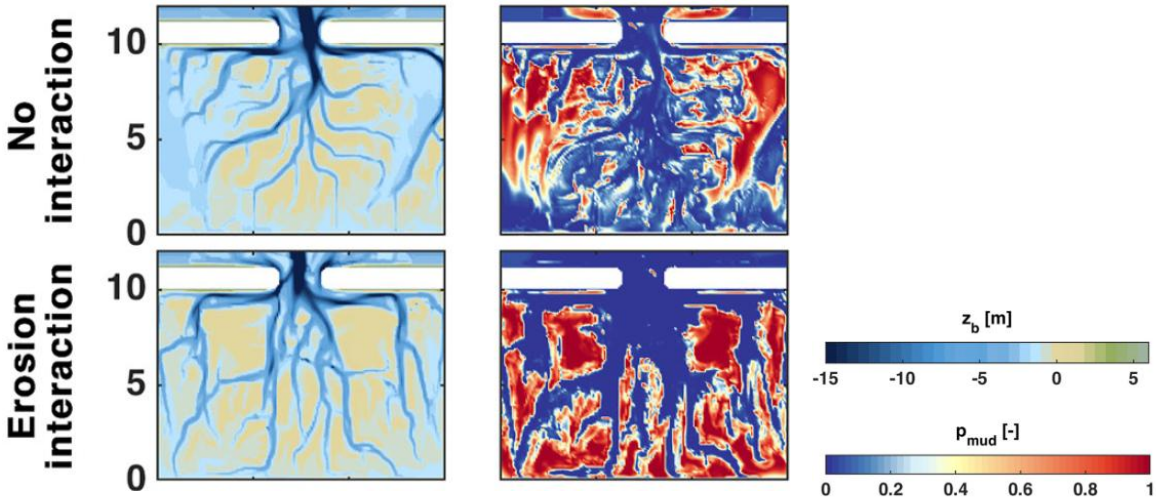

Figure 17. Morphodynamic and bed composition simulation results that highlight effect of sand-mud interaction on erosion (Colina Alonso et al., 2023)

5. CONCLUSIONS AND KNOWLEDGE GAPS

5.1. CONCLUSIONS

Based on this review, we endeavor to answer the literature research questions posed in Chapter 2.

How to define sand-mud and what are systems that contain sand-mud?

Sand-mud are characterized by the percentage of each sediment fraction (e.g. sand, clay, and silt). Classification is based on size and physical properties of each sediment component. Sand is a non-cohesive particle whose transport is governed by its size and weight. Clay is a cohesive particle that is governed by its electrochemical interactive forces. Finally, silt is a non-cohesive particle with an apparent cohesive property due to permeability.

Sand-mud is typically found in estuaries. Various estuaries around the world contain sand-mud albeit with different types of mud. Some estuaries contain more clayey mud while others, are siltier. A lot of research and engineering works were done in these places because of the economic and ecological value they provide.

The Scheldt estuary, and the Wadden sea are sand-mud systems with significant clay content that have been modeled using Delft3D. Extensive research has been done on these systems which results in a better understanding of the model input parameters for sand-mud erosion.

The Yangtze estuary and Mekong delta are sand-mud systems with significant silt content that are the study sites of a large body of research. These modeling exercises have yielded results comparable to measured field data in terms of morphodynamics and suspended sediment concentration. However, the input parameters used in the model are used as calibration parameters. It appears that the input parameters were chosen either for how acceptable the morphodynamic results came out or if the parameters fell into the range of acceptable values.

Comparative studies have also compared and contrasted different sand-mud systems. Initial comparative studies emphasize the role of the dominant hydrodynamics on a global scale. More recent work used different sand-mud ratios in morphodynamic modeling. Neither of these approaches have taken into account the erosion processes of each sediment component, i.e. sand, clay and silt.

What are the physical processes in sand-mud transport and which of these processes are modeled mathematically?

Sand-mud beds erode when bed shear stress exceeds a threshold called critical bed shear stress. The erosion rate of sand-mud into the water column is then estimated in a form similar to the Partheniades erosion formula. This formulation has two independent parameters: critical bed shear stress, τ_{cr}, and the erosion parameter, M. The critical bed shear stress has been described by many researches each stemming from their own experiments and datasets. The critical bed shear stress has been described using the bulk density, median grain size, or mass fraction of mud. Because these formulations are site- or dataset-specific, a critical bed shear stress equation that covers all combinations of sand-silt-clay does not exist. The erosion parameter, M, is not often the topic of research. Some morphodynamic modeling use this parameter more for calibration than a result of geotechnical parameters. An M parameter for clay and silt have been proposed but not widely accepted in the literature. Further, neither of these parameters have mathematical formulas that cover the entire sand-silt-clay trio. Finally, among the research that describes sand-mud erosion, Van Ledden (2003) proposes a framework that characterizes sand-mud beds as either non-cohesive or cohesive depending on the mass fraction of mud compared to a pre-defined critical mud content.

As sand-mud particles slowly descend back towards the bed, a natural segregation occurs as larger and heavier particles settle before smaller and lighter ones. However, due to the different settling rates,

the sediment concentration along portions of the water column saturate. This saturation leads to the so-called hindered settling. This phenomena is well described and accepted by the literature.

The deposition of sand-mud particles back into the bed is estimated using the Krone formulation. Some modifications have been done on this formulation to account for other processes such as break-up or strength development of flocs or resolution of water columns in numerical models. When sand-mud particles are on the bed, water is expelled between the particles. This is the consolidation of sand-mud beds. Attempts have been made to incorporate this in RANS models but in general, sand-mud morphodynamic modeling does not take this into account.

How is sand-mud bed evolution modeled in the RANS hydro-morphodynamic software, Delft3D?
Delft3D solves the non-linear shallow water equations with different closure models and computes the boundary layer hydrodynamics using different formulations. Numerically, this model uses a finite difference scheme or finite element scheme depending on whether a structured or an unstructured grid is used, respectively.

The morphodynamic scheme uses different sediment fractions to describe the different transport loads. Multiple fractions can be defined to describe different sand and mud. A morphological factor, MorFac, is also implemented in the scheme to hasten morphologic change. These two features of Delft3D provide the flexibility to model morphodynamic changes to different types of systems.

Additionally, Delft3D implemented a fluff layer to describe fresh mud deposits on top of the bed. This layer is always on top and can be set with different sediment properties such as critical bed shear stress, and erosion parameter. This fluff layer model combined with the framework of Van Ledden (2003) to describe the nature of sand-mud beds provides a more realistic representation of sand-mud morphodynamics.

Each of these features have been used in previous literature that utilized Delft3D in morphodynamic modeling. These modeling examples show different types of sand-mud beds but also different ways of using these features. The results of these morphodynamic modeling exercises are comparable to the field data. This demonstrates the ability of the morphodynamic scheme of Delft3D to replicate the processes in sand-mud bed evolution.

5.2. KNOWELDGE GAPS

The following knowledge gaps come into focus as a result from the literature review and its conclusions.

The erosion processes of sand, silt, and clay are not incorporated in a generic sand-mud bed erosion formula.
For sand-mud beds, it is accepted in the literature to describe the erosion process using the Partheniades erosion formulation. This equation uses two independent parameters: the critical bed shear stress, and the erosion parameter, M.

Previous research has shown that sand-mud systems with either significant clay or silt content have different processes both at initiation of motion (described by the critical bed shear stress) and during erosion (which is a function of the erosion parameter). At present, these processes are not included to provide a generic formulation for sand-mud erosion.

The effect of accounting for the processes of silt in the numerical modeling of decadal estuarine morphodynamics is largely unknown.
There is a plethora of research that used the model Delft3D to simulate decadal estuarine

morphodynamics of silt-dominated systems. These systems include the Yangtze Estuary and the Mekong delta.

The work by te Slaa (2020) and Yao et al. (2022) highlighted the process of silt erosion. Both works proposed formulations to estimate the critical bed shear strength of silty beds while te Slaa also proposed an equation to estimate the erosion parameter, M, for silt beds. These formulations have not been utilized to estimate time- or spatially-varying critical bed shear stress. The calculation of these erosion parameters gives the opportunity to explicitly incorporate the erosion processes of silt into a model like Delft3D.

The differences in resilience to sea level rise between sand-mud systems with either significant clay or silt content are not clear.
Comparative studies have distinguished between different types of dominant hydrodynamics on long-term estuary bed evolution. Recently, the work by Jiang et al. (2024) shows the effect of incorporating the correct bed characteristics in long-term morphodynamics.

Further, estuaries have also been the subject of sea level rise research to investigate the potential effect on future morphodynamics. With our current understanding of morphodynamic modeling and potential sea level rise, a gap exists to investigate the response of estuaries to sea level rise with different sediment compositions.

6. REFERENCES

Allersma, E. (1988). *Morfologisch onderzoek Noordelijk Deltabekken. Morfologische modellering deel IV: Composition and Density of Sediments (in Dutch) (Report Z71.03)*.

ASTM D7928-21e1. (2021). *Standard Test Method for Particle-Size Distribution (Gradation) of Fine-Grained Soils Using the Sedimentation (Hydrometer) Analysis*.

Bolle, A., Bing Wang, Z., Amos, C., & De Ronde, J. (2010). The influence of changes in tidal asymmetry on residual sediment transport in the Western Scheldt. *Continental Shelf Research*, *30*(8), 871–882. https://doi.org/10.1016/j.csr.2010.03.001

Bosboom, J., & Stive, M. (2021). *Coastal Dynamics*. TU Delft Open. https://doi.org/10.5074/T.2021.001

Chen, W., Ban, H., Mao, C., Liang, H., & Jiang, M. (2024). Sediment Dynamics Subject to Sea Level Rise in the Yangtze River Estuary. *Journal of Ocean University of China*, *23*(6), 1572–1582. https://doi.org/10.1007/s11802-024-5741-7

Colina Alonso, A., van Maren, D. S., Herman, P. M. J., van Weerdenburg, R. J. A., Huismans, Y., Holthuijsen, S. J., Govers, L. L., Bijleveld, A. I., & Wang, Z. B. (2022). The Existence and Origin of Multiple Equilibria in Sand-Mud Sediment Beds. *Geophysical Research Letters*, *49*(22). https://doi.org/10.1029/2022GL101141

Colina Alonso, A., van Maren, D. S., van Weerdenburg, R. J. A., Huismans, Y., & Wang, Z. B. (2023). Morphodynamic modelling of tidal basins: The role of sand-mud interaction. *Journal of Geophysical Research: Earth Surface*. https://doi.org/10.1029/2023jf007391

Cuthbertson, A. J. S., Samsami, F., & Dong, P. (2018). Model studies for flocculation of sand-clay mixtures. *Coastal Engineering*, *132*, 13–32. https://doi.org/10.1016/j.coastaleng.2017.11.006

Dam, G., van der Wegen, M., Labeur, R. J., & Roelvink, D. (2016). Modeling centuries of estuarine morphodynamics in the Western Scheldt estuary. *Geophysical Research Letters*, *43*(8), 3839–3847. https://doi.org/10.1002/2015GL066725

Dean, R. G., & Dalrymple, R. A. (2001). *Coastal Processes with Engineering Applications*. Cambridge University Press. https://doi.org/10.1017/CBO9780511754500

Deltares. (2023). *Delft3D 3D/2D modelling suite for integral water solutions User Manual*. https://content.oss.deltares.nl/delft3d4/Delft3D-FLOW_User_Manual.pdf

DHI. (2024). *MIKE 21 & MIKE 3 Flow Model FM: Mud Transport Module*. https://manuals.mikepoweredbydhi.help/latest/Coast_and_Sea/MIKE_213_MT_FM_ScientificDoc.pdf

Dissanayake, D. M. P. K., Roelvink, J. A., & van der Wegen, M. (2009). Modelled channel patterns in a schematized tidal inlet. In *Coastal Engineering* (Vol. 56, Issues 11–12, pp. 1069–1083). https://doi.org/10.1016/j.coastaleng.2009.08.008

Einstein, H. A., & Krone, R. B. (1962). Experiments to determine modes of cohesive sediment transport in salt water. *Journal of Geophysical Research*, *67*(4), 1451–1461. https://doi.org/10.1029/JZ067i004p01451

Elias, E. P. L., Van Der Spek, A. J. F., Wang, Z. B., Cleveringa, J., Jeuken, C. J. L., Taal, M., & Van Der Werf, J. J. (2023). Large-scale morphological changes and sediment budget of the Western Scheldt estuary 1955-2020: the impact of large-scale sediment management. In *Geologie en Mijnbouw/Netherlands Journal of Geosciences* (Vol. 102, Issues 1–3). Cambridge University Press. https://doi.org/10.1017/njg.2023.11

Elmilady, H., van der Wegen, M., Roelvink, D., & van der Spek, A. (2022). Modeling the Morphodynamic Response of Estuarine Intertidal Shoals to Sea-Level Rise. *Journal of Geophysical Research: Earth Surface*, *127*(1). https://doi.org/10.1029/2021JF006152

Feng, H., Tang, L., Wang, Y., Guo, C., Liu, D., Zhao, H., Zhao, L., & Wang, W. J. (2020). Effects of recent morphological change on the redistribution of flow discharge in the Yangtze River Delta. *Continental Shelf Research*, *208*. https://doi.org/10.1016/j.csr.2020.104218

Fettweis, M., Francken, F., Van den Eynde, D., Verwaest, T., Janssens, J., & Van Lancker, V. (2010). Storm influence on SPM concentrations in a coastal turbidity maximum area with high anthropogenic impact (southern North Sea). *Continental Shelf Research*, *30*(13), 1417–1427.

https://doi.org/10.1016/j.csr.2010.05.001
Galloway, W. (1975). Process framework for describing the morphologic and stratigraphic evolution of deltaic depositional system. *Society of Economic Paleontologists and Mineralogist (SEPM), Special Publication No. 31*, 127–156.
Guo, L., van der Wegen, M., Roelvink, D. (J. A.), Wang, Z. B., & He, Q. (2015). Long-term, process-based morphodynamic modeling of a fluvio-deltaic system, part I: The role of river discharge. *Continental Shelf Research*, *109*, 95–111. https://doi.org/10.1016/j.csr.2015.09.002
Jacobs, W., Le Hir, P., Van Kesteren, W., & Cann, P. (2011). Erosion threshold of sand–mud mixtures. *Continental Shelf Research*, *31*(10), S14–S25. https://doi.org/10.1016/j.csr.2010.05.012
Jacobs, Walter. (2011). *Sand-mud erosion from a soil mechanical perspective.* [Doctoral thesis, Delft University of Technology]. https://repository.tudelft.nl/islandora/object/uuid%3A6d908f04-14fd-47f3-b292-af4b99a8fb11
Jiang, C. H., Zhou, Z., Townend, I. H., Guo, L. C., Wei, Y. Z., Luo, F., & Zhang, C. K. (2024). Modelling the impact of sediment composition on long-term estuarine morphodynamics. *Coastal Engineering*, *193*. https://doi.org/10.1016/j.coastaleng.2024.104595
Kuang, C., Chen, W., Gu, J., Su, T. C., Song, H., Ma, Y., & Dong, Z. (2017). River discharge contribution to sea-level rise in the Yangtze River Estuary, China. *Continental Shelf Research*, *134*, 63–75. https://doi.org/10.1016/j.csr.2017.01.004
Kuang, C., Liu, X., Gu, J., Guo, Y., Huang, S., Liu, S., Yu, W., Huang, J., & Sun, B. (2013). Numerical prediction of medium-term tidal flat evolution in the Yangtze Estuary: Impacts of the Three Gorges project. *Continental Shelf Research*, *52*, 12–26. https://doi.org/10.1016/j.csr.2012.10.006
Luo, W., Shen, F., He, Q., Cao, F., Zhao, H., & Li, M. (2022). Changes in suspended sediments in the Yangtze River Estuary from 1984 to 2020: Responses to basin and estuarine engineering constructions. *Science of the Total Environment*, *805*. https://doi.org/10.1016/j.scitotenv.2021.150381
Manning, A. J., Baugh, J. V., Spearman, J. R., Pidduck, E. L., & Whitehouse, R. J. S. (2011). The settling dynamics of flocculating mud-sand mixtures: Part 1-Empirical algorithm development. *Ocean Dynamics*, *61*(2–3), 311–350. https://doi.org/10.1007/s10236-011-0394-7
Manning, A. J., Baugh, J. V., Spearman, J. R., & Whitehouse, R. J. S. (2010). Flocculation settling Characteristics of mud: Sand mixtures. *Ocean Dynamics*, *60*(2), 237–253. https://doi.org/10.1007/s10236-009-0251-0
Mehta, A. J. (1988). Laboratory Studies on Cohesive Sediment Deposition and Erosion. In *Physical Processes in Estuaries* (pp. 427–445). Springer Berlin Heidelberg. https://doi.org/10.1007/978-3-642-73691-9_21
Meyer-Peter, E., & Müller, R. (1948). Formulas for bed-load transport. *IAHR*, 39–64.
Mikeš, D., & Manning, A. J. (2010). Assessment of Flocculation Kinetics of Cohesive Sediments from the Seine and Gironde Estuaries, France, through Laboratory and Field Studies. *Journal of Waterway, Port, Coastal, and Ocean Engineering*, 295–358. https://doi.org/10.1061/ASCEWW.1943-5460.0000053
Mitchener, H., Torfs, H., & Whitehouse, R. (1997). Erosion of mud/sand mixtures [Coastal Eng., 29 (1996) 1–25]. *Coastal Engineering*, *30*(3–4), 319. https://doi.org/10.1016/S0378-3839(97)00002-1
Nienhuis, J. H., Ashton, A. D., Edmonds, D. A., Hoitink, A. J. F., Kettner, A. J., Rowland, J. C., & Törnqvist, T. E. (2020). Global-scale human impact on delta morphology has led to net land area gain. *Nature*, *577*(7791), 514–518. https://doi.org/10.1038/s41586-019-1905-9
Partheniades, E. (1965). Erosion and Deposition of Cohesive Soils. *Journal of the Hydraulics Division*, *91*(1), 105–139. https://doi.org/10.1061/JYCEAJ.0001165
Roberts, J., Jepsen, R., Gotthard, D., & Lick, W. (1998). Effects of Particle Size and Bulk Density on Erosion of Quartz Particles. *Journal of Hydraulic Engineering*, *124*(12), 1261–1267. https://doi.org/10.1061/(ASCE)0733-9429(1998)124:12(1261)
Schwarz, C., Cox, T., van Engeland, T., van Oevelen, D., van Belzen, J., van de Koppel, J., Soetaert, K., Bouma, T. J., Meire, P., & Temmerman, S. (2017). Field estimates of floc dynamics and settling velocities in a tidal creek with significant along-channel gradients in velocity and SPM. *Estuarine,*

Coastal and Shelf Science, *197*, 221–235. https://doi.org/10.1016/j.ecss.2017.08.041
Shields, A. (1936). *Application of Similarity Principles and Turbulence Research to Bed-Load Movement*. https://authors.library.caltech.edu/25992/1/Sheilds.pdf
te Slaa, S. (2020). *Deposition and erosion of silt-rich sediment-water mixtures* [Doctoral thesis, Delft University of Technology]. https://doi.org/https://doi.org/10.4233/uuid:c50eb76c-b2ea-49cf-9873-5c929ff496dc
TELEMAC.org. (2022). *GAIA UserManual Version v8p4*.
TELEMAC.org. (2023). *TELEMAC-3D UserManual*. https://www.opentelemac.org/
Torfs, H. (1995). *EROSION OF MUD/SAND MIXTURES*.
Tu, L. X., Thanh, V. Q., Reyns, J., Van, S. P., Anh, D. T., Dang, T. D., & Roelvink, D. (2019). Sediment transport and morphodynamical modeling on the estuaries and coastal zone of the Vietnamese Mekong Delta. *Continental Shelf Research*, *186*, 64–76. https://doi.org/10.1016/j.csr.2019.07.015
Unverricht, D., Szczuciński, W., Stattegger, K., Jagodziński, R., Le, X. T., & Kwong, L. L. W. (2013). Modern sedimentation and morphology of the subaqueous Mekong Delta, Southern Vietnam. *Global and Planetary Change*, *110*, 223–235. https://doi.org/10.1016/j.gloplacha.2012.12.009
Van Der Wegen, M., & Roelvink, J. A. (2008). Long-term morphodynamic evolution of a tidal embayment using a two-dimensional, process-based model. *Journal of Geophysical Research: Oceans*, *113*(3). https://doi.org/10.1029/2006JC003983
van der Wegen, M., & Roelvink, J. A. (2012). Reproduction of estuarine bathymetry by means of a process-based model: Western Scheldt case study, the Netherlands. *Geomorphology*, *179*, 152–167. https://doi.org/10.1016/j.geomorph.2012.08.007
van Ledden, M. (2002). *A process-based sand-mud model* (pp. 577–594). https://doi.org/10.1016/S1568-2692(02)80041-9
Van Ledden, M. (2003). Sand-mud segregation in estuaries and tidal basins [Doctoral thesis, Delft University of Technology]. In *Communications on Hydraulic and Geotechnical Engineering*. http://resolver.tudelft.nl/uuid:b3d2d558-7f80-455a-be8a-5a8a6a8dbd21
Van Ledden, M., Van Kesteren, W. G. M., & Winterwerp, J. C. (2004). A conceptual framework for the erosion behaviour of sand-mud mixtures. *Continental Shelf Research*, *24*(1), 1–11. https://doi.org/10.1016/j.csr.2003.09.002
van Maren, D. S., Vroom, J., Fettweis, M., & Vanlede, J. (2020). Formation of the Zeebrugge coastal turbidity maximum: The role of uncertainty in near-bed exchange processes. *Marine Geology*, *425*. https://doi.org/10.1016/j.margeo.2020.106186
van Maren, D. S., Winterwerp, J. C., Wu, B. S., & Zhou, J. J. (2009). Modelling hyperconcentrated flow in the Yellow River. *Earth Surface Processes and Landforms*, *34*(4), 596–612. https://doi.org/10.1002/esp.1760
Van Prooijen, B. C., & Winterwerp, J. C. (2010). A stochastic formulation for erosion of cohesive sediments. *Journal of Geophysical Research: Oceans*, *115*(1). https://doi.org/10.1029/2008JC005189
van Rijn, L. (1993). *Principles of Sediment Transport in Rivers, Estuaries and Coastal Seas*. Aqua Publications.
van Rijn, L. C. (2007a). Unified View of Sediment Transport by Currents and Waves. I: Initiation of Motion, Bed Roughness, and Bed-Load Transport. *Journal of Hydraulic Engineering*, *133*(6), 649–667. https://doi.org/10.1061/(ASCE)0733-9429(2007)133:6(649)
van Rijn, L. C. (2007b). Unified View of Sediment Transport by Currents and Waves. II: Suspended Transport. *Journal of Hydraulic Engineering*, *133*(6), 668–689. https://doi.org/10.1061/(ASCE)0733-9429(2007)133:6(668)
van Rijn, L. C. (2020). Erodibility of Mud–Sand Bed Mixtures. *Journal of Hydraulic Engineering*, *146*(1). https://doi.org/10.1061/(asce)hy.1943-7900.0001677
van Rijn, L. C., & Barth, R. (2019). Settling and Consolidation of Soft Mud–Sand Layers. *Journal of Waterway, Port, Coastal, and Ocean Engineering*, *145*(1). https://doi.org/10.1061/(asce)ww.1943-5460.0000483
Wang, X., Zhang, W., Xie, X., Chen, H., & Chen, B. (2024). Holocene sedimentary distribution and

morphological characteristics reworked by East Asian monsoon dynamics in the Mekong River shelf, South Vietnam. *Estuarine, Coastal and Shelf Science*, *302*. https://doi.org/10.1016/j.ecss.2024.108784

Wang, Z. B., Jeuken, M. C. J. L., Gerritsen, H., de Vriend, H. J., & Kornman, B. A. (2002). Morphology and asymmetry of the vertical tide in the Westerschelde estuary. *Continental Shelf Research*, *22*(17), 2599–2609. https://doi.org/10.1016/S0278-4343(02)00134-6

Wentworth, C. K. (1922). A Scale of Grade and Class Terms for Clastic Sediments. *The Journal of Geology*, *30*(5), 377–392. https://doi.org/10.1086/622910

Winterwerp, J. C. (1998). A simple model for turbulence induced flocculation of cohesive sediment. *Journal of Hydraulic Research*, *36*(3), 309–326. https://doi.org/10.1080/00221689809498621

Winterwerp, J. C., Kessel, T. van, Maren, D. S. van, & Prooijen, B. C. van. (2021). *Fine Sediment in Open Water* (Vol. 55). WORLD SCIENTIFIC. https://doi.org/10.1142/12473

Winterwerp, J. C., Manning, A. J., Martens, C., de Mulder, T., & Vanlede, J. (2006). A heuristic formula for turbulence-induced flocculation of cohesive sediment. *Estuarine, Coastal and Shelf Science*, *68*(1), 195–207. https://doi.org/10.1016/j.ecss.2006.02.003

Winterwerp, J. C., & van Kesteren, W. G. M. (2004). *INTRODUCTION TO THE PHYSICS OF COHESIVE SEDIMENT IN THE MARINE ENVIRONMENT*. Elsevier B.V. http://www.clscvicr.com/locatc/pcrmissions

Wu, W., Perera, C., Smith, J., & Sanchez, A. (2018). Critical shear stress for erosion of sand and mud mixtures. *Journal of Hydraulic Research*, *56*(1), 96–110. https://doi.org/10.1080/00221686.2017.1300195

Xu, C., Odum, B., Chen, Y., & Yao, P. (2022). Evaluation of the Role of Silt Content on the Flocculation Behavior of Clay-Silt Mixtures. *Water Resources Research*, *58*(11). https://doi.org/10.1029/2021WR030964

Yamada, F., & Kobayashi, N. (2003). *Parameterization of Mudflat Profile Changes caused by Seasonal Tide Level Variations*. https://bpb-us-w2.wpmucdn.com/sites.udel.edu/dist/0/7241/files/2018/03/CACR-03-02-238va84.pdf

Yao, P., Su, M., Wang, Z., van Rijn, L. C., Stive, M. J. F., Xu, C., & Chen, Y. (2022). Erosion Behavior of Sand-Silt Mixtures: Revisiting the Erosion Threshold. *Water Resources Research*, *58*(9). https://doi.org/10.1029/2021WR031788

Zhao, L., Xin, P., Cheng, H., & Chu, A. (2023). Change of turbidity maximum in Yangtze Estuary after construction of the Three Gorges Dam. *Continental Shelf Research*, *258*. https://doi.org/10.1016/j.csr.2023.104983

Zhu, C., van Maren, D. S., Guo, L., Lin, J., He, Q., & Wang, Z. B. (2021). Effects of Sediment-Induced Density Gradients on the Estuarine Turbidity Maximum in the Yangtze Estuary. *Journal of Geophysical Research: Oceans*, *126*(5). https://doi.org/10.1029/2020JC016927